

Surface plasmon mediated emission in resonant-cavity light-emitting diodes

P. A. Porta,^{a)} M. Harries, and H. D. Summers

School of Physics and Astronomy, Cardiff University, Cardiff, Wales CF24 3YB, United Kingdom

(Received 13 January 2006; accepted 9 August 2006; published online 22 September 2006)

In this letter the authors describe a particular method to outcouple in air, via surface plasmons (SPs), optical radiation trapped in leaky waveguide modes of a resonant-cavity light-emitting diode. The deposition of a thin metal layer on the device surface creates SP modes at both the metal-dielectric interfaces. The successive overcoating of the metal layer with a thin polymer film and the roughening of its surface produce outcoupling of radiation trapped in leaky modes via SP modes. Experimental results for polarization resolved reflectivity and emission spectra are in excellent agreement with theoretical predictions. © 2006 American Institute of Physics.

[DOI: 10.1063/1.2357034]

Surface plasmons (SPs) are transverse-magnetic (TM) waves supported by electron gas oscillations at a metal-dielectric interface. In the case of a smooth interface the dispersion relation that defines SP modes lies below the light line $\omega = ck$, with ω the electromagnetic wave frequency, c its speed in vacuum, and k its propagation vector.¹ For this reason SP modes cannot radiate and usually are described as evanescent waves decaying away rapidly from the metal-dielectric interface. In very thin metal films bounded by two dielectric materials the two SP waves at each metal-dielectric interface can couple to form a new type of mode called coupled SP mode that can favor transfer of energy from one medium into the other.² The extraction of optical radiation from light sources using SP modes requires a method to change the SP momentum to make it radiative. The formation of diffraction gratings on the surface of an organic light-emitting diode³ (LED) and the definition of a periodic pattern of submicron holes in the top layer of a semiconductor LED are two possible solutions to outcouple SP modes in air.⁴ A hemispherical prism is also another useful tool to extract surface plasmon coupled emission⁵ from fluorescent dye molecules 20–250 nm away from a metal surface.

In this letter we describe a simple method to outcouple, via SP modes, optical radiation trapped inside a particular light source called resonant-cavity LED (RCLED). This extraction scheme requires only a thin gold layer with a rough surface and a very thin overcoating of a polymer called polymethylmethacrylate (PMMA). The realization of this type of device has been motivated by the growing interest in developing new surface sensitive biosensors.⁶ There are several techniques to immobilize biological and biochemical samples on a surface of a biosensor.⁷ The availability of a light source whose output properties change in a controlled way depending on the substance present on its surface would allow for the realization of a new compact SP based biosensor with integrated illumination.

The RCLED is a semiconductor LED whose active region is embedded in a one-wavelength cavity to resonantly enhance its optical emission.⁸ As can be seen in Fig. 1, this device is formed by two distributed Bragg reflector (DBR) produced by alternating several pairs of $\lambda/4$ layers of $\text{Al}_{0.5}\text{Ga}_{0.5}\text{As}$ and AlAs . They define a 1λ cavity containing

the active region composed of three GaInP/AlGaInP quantum wells with peak emission wavelength at 645 nm. The emission modes of the RCLED can be divided in three categories: Fabry-Pérot modes, leaky modes, and guided modes.⁹ Fabry-Pérot modes are defined by the cavity resonance; they are emitted from the top of the device and their angular emission is limited by the critical angle θ_c for total internal reflection between the semiconductor material and the external medium where these modes radiate. Guided modes are determined by the waveguiding properties of this structure in the direction parallel to the epitaxial plane; they are confined in the active region of the device and are emitted only from its side. Leaky modes are created by the particular structure of the DBR and are usually an unwanted loss in a standard RCLED. Light tends to propagate in the region where the refractive index is the largest.¹⁰ Since GaAs and $\text{Al}_{0.5}\text{Ga}_{0.5}\text{As}$ have refractive index higher than that of AlGaInP, part of the optical radiation generated in the active region is coupled into these layers of the DBR forming leaky modes towards the surface or the substrate of the device. The epitaxial structure of the RCLEDs for this project is terminated by a 10 nm thin cap layer of GaAs used normally to define via anodic oxidation insulating regions on the top of the device.¹¹ In the devices made for this project the cap layer is left unoxidized. Optical radiation in leaky modes is guided efficiently underneath the RCLED surface where it can interact with surface modes, as shown in the sketch of Fig. 1, and be outcoupled into air.

Since our final goal is to develop a new surface sensor for biological and biochemical substances deposited on the top of the device, we process large area samples, typically $5 \times 5 \text{ mm}^2$, whose emission can be easily analyzed with an optical fiber or a charge coupled device camera. Due to their large size, these devices can be considered as one-dimensional resonators in the direction orthogonal to the epitaxial plane. To fabricate these devices we deposited 50 nm of gold over the entire top surface of the chip using a thin Cr layer (2–4 nm) to improve the gold adhesion to the semiconductor surface. The metallization covered the entire surface of the emitting device to produce uniform current injection and was followed by thermal annealing at 385° in a nitrogen atmosphere. This process improved the p -type Ohmic contact and created the surface roughening¹² that made possible outcoupling of SP modes in the dielectric

^{a)}Electronic mail: portapa@cf.ac.uk

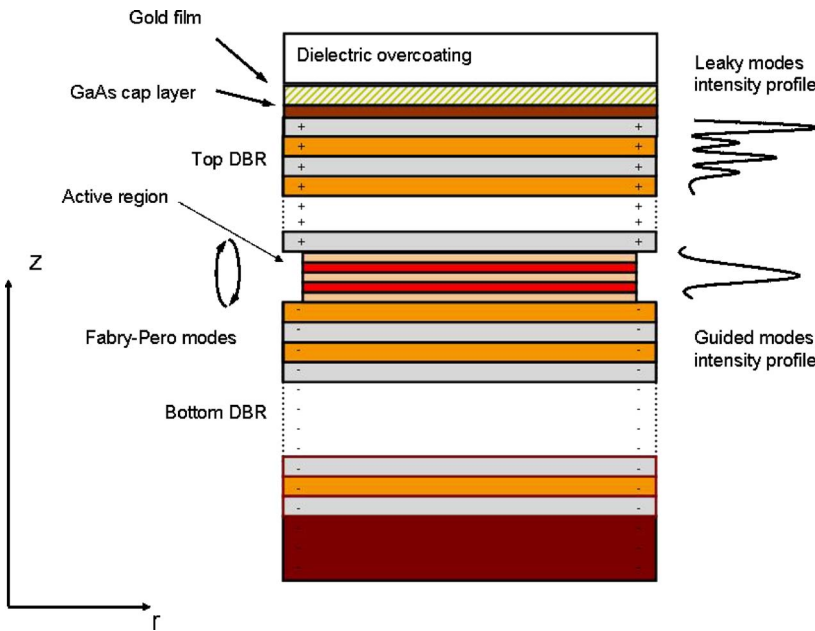


FIG. 1. (Color online) Schematic representation of the multilayer structure of a RCLED. The z axis defines the vertical direction of growth of the multilayer structure while the r axis defines the epitaxial plane where the SP modes lie. The active region, represented by the narrower part of the drawing, is sandwiched between two DBRs. The top DBR has a capping layer made of GaAs where the gold layer is deposited. The dielectric overcoating is PMMA. The three types of optical emission from a RCLED are represented schematically and are explained in detail in this letter.

medium.¹ The metal layer generated SP modes at both the metal-dielectric interfaces and was thin enough to allow for interaction between SP modes at the top metal-dielectric interface with leaky modes at the semiconductor surface.

In Fig. 2 we have merged two images of the surface of the thin gold layer deposited onto GaAs before (picture on the left) and after (picture on the right) thermal annealing. These images, taken with a scanning electron microscope, show clearly how thermal annealing, as reported in Ref. 12, causes the formation of nanometer scale metal islands that transform drastically the structure of the metal surface. In the 1970s it was demonstrated that the formation of a thin dielectric layer on the top of a metal could alter the SP resonance properties.¹³ Following these results we deposited a thin coating made of 200 nm of PMMA over the gold layer to study its effects on the SP's optical properties and consequently on the device optical output. Three small regions with size of $0.5 \times 0.5 \text{ mm}^2$ on one side of the device were left uncoated to provide a direct comparison of the effects produced by the dielectric coating.

The first analysis consisted of taking polarization resolved reflectivity measurements of parts of the device with and without PMMA at different angles of incidence. Two TM polarized reflectivity spectra taken at 70° with respect to the normal to the surface are shown in Fig. 3. The bottom curve corresponding to a region covered with PMMA shows a clear dip in the reflectivity at $0.55 \mu\text{m}$ which we attribute to coupling of the incident radiation with SP modes at the metal-dielectric interface via surface roughness. To model this process and verify the validity of this assumption we have calculated the k vectors of the SP k_{sp} given by the dispersion relation for an air-dielectric-metal film system:⁹

$$\varepsilon_m k_2 [1 + r(k) \exp(-2k_2 t)] + \varepsilon_d k_3 [1 - r(k) \exp(-2k_2 t)] = 0, \quad (1)$$

with

$$r(k) = (\varepsilon_d k_1 - k_2) / (\varepsilon_d k_1 + k_2). \quad (2)$$

The k vectors k_i are defined as $k_1^2 = (k^2 - k_0^2)$ in air, $k_2^2 = (k^2 - \varepsilon_d k_0^2)$ in the dielectric medium, and $k_3^2 = (k^2 - \varepsilon_m k_0^2)$ in the metal film. The permittivities of the dielectric medium and of

the metal film are, respectively, ε_d and ε_m while t is the thickness of the dielectric layer.

The solutions of Eq. (1) are used to verify the validity of the in-plane momentum conservation at the metal surface for a wave incident at an angle θ with respect to the normal expressed by

$$k \sin(\theta) + k_r = k_{\text{sp}}. \quad (3)$$

The terms k_{sp} and k_r are the moduli of the SP mode k vector and of the k vector representing the scattering induced by surface roughness.

Since the k vector of the incident radiation and its incidence angle θ are known and k_{sp} can be calculated using Eq. (1), Eq. (3) allows one to calculate the average k vector k_r . At the wavelength of $0.55 \mu\text{m}$, k_r is found to be equal to $9.4 \mu\text{m}^{-1}$, in good agreement with typical values of the roughness period of metal surfaces reported in the literature.¹⁴ Modeling surface roughness of a metal layer is usually done using a spectral density function $s(k)$ that gives values and ranges of the momentum that can be transferred into photons.¹ The irregularity of a rough surface broadens

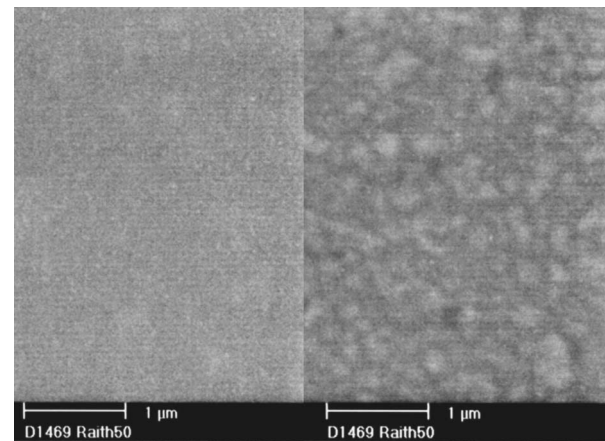


FIG. 2. Scanning electron microscope images of Au surface not annealed (left) and annealed at 385° for 5 min in nitrogen atmosphere (right).

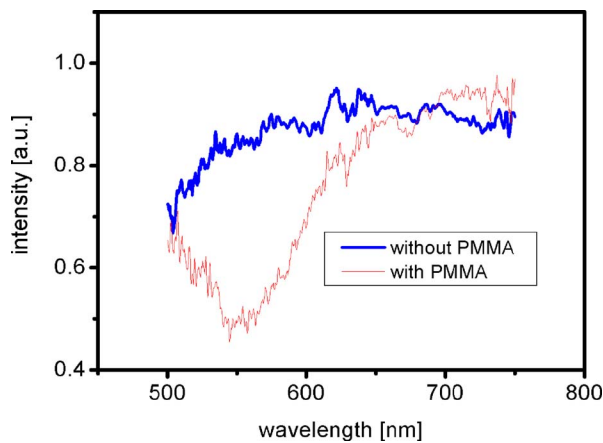


FIG. 3. (Color online) TM polarized reflectivity spectra of a region uncoated (thick line) and of a region coated (thin line) with PMMA at an angle of observation equal to 70° .

the spectral function $s(k)$. Hence it has a specific spectral width Δk_r that can be calculated using Eq. (3). By taking the k vector corresponding to the reflectivity cut off at about $0.68 \mu\text{m}$ in Fig. 3 and the k vector of the SP mode at this wavelength, the value of Δk_r was found to be equal to $3.3 \mu\text{m}^{-1}$.

The emission spectra from these devices have been collected with an optical fiber close to the surface of the device and connected to an optical spectrum analyzer ANDO AQ6315. The thick lines in the inset of Fig. 4 represent emission from parts coated with PMMA and the thin line emission from parts uncoated. The RCLED output emission depends on the direction of observation⁷ and has a maximum at the angle at which the frequency of the resonant Fabry-Perot mode coincides with that of the peak gain of the active medium. The spectra have been normalized to the emission values at normal incidence since our interest is only in the quantification of the relative enhancement mediated by SP modes. As can be seen by comparing these data, the relative enhancement starts at 30° and reaches a maximum of about 40% at an angle equal to 50° . In the main part of Fig. 4 we have plotted the ratios of the spectral peak intensities from

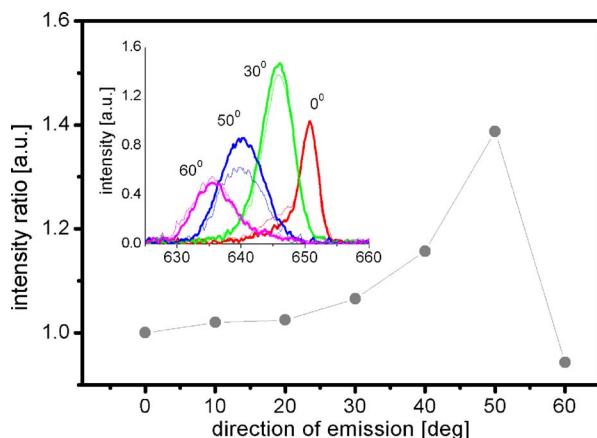


FIG. 4. (Color online) Peak intensity ratios of emission from regions coated with PMMA and uncoated. Inset: emission spectra from regions of the RCLED surface uncoated (thin lines) and coated (thick lines) with PMMA.

regions with and without PMMA at various angles of observation to show clearly the maximum enhancement at 50° . By using Eq. (3) for the conservation of momentum at the wavelength of $0.64 \mu\text{m}$, with the k vector k_{sp} of the SP calculated using Eq. (1) and the k vector k_r of the surface roughness calculated from the reflectivity data, the angle of maximum emission in air is found to be equal to 49° , in good agreement with the data in Fig. 3. By using Eq. (3) and replacing the k vector of the surface roughness with the sum of k_r and its bandwidth Δk_r , the minimum angle of emission into air can be found to be equal to 26° , again in good agreement with the experimental data. When the angle of emission into the PMMA reaches the value of 41.8° , the angle of total internal reflection for the interface PMMA-air, light scattered from SP modes cannot be outcoupled directly into air anymore.

The beam shape of this set of RCLEDs is doughnutlike since there is detuning between the cavity resonance and the peak gain of the active medium.⁹ The top emission from the device coated with PMMA is altered to produce a wider ring of emission due to the enhanced intensity at 50° . By bringing the optical fiber close to the cleaved facets of the devices, it is possible to measure a decrease of the side emission from regions coated with PMMA in correspondence with the enhancement of their top emission. This decrease of optical emission is found to be in a spectral range that contains the TM polarized leaky modes that are outcoupled on the top of the device by the nanostructure.

To conclude, we have demonstrated that the deposition of a thin dielectric layer on the gold coated surface of a RCLED modifies its emission through outcoupling of optical radiation via SP modes. This emission enhancement is in a direction determined by the momentum matching between photon, surface plasmon, and the effective grating formed by the rough Au surface. This device has potential application as a SP based biosensor for biological samples immobilized on its upper surface.

The authors wish to acknowledge the Wellcome Trust for financial support (Grant No. 072640/Z/03/Z) and Glyn Summers for his precious help to prepare various experimental setups.

¹H. Raether, *Surface Plasmon on Smooth and Rough Surfaces and on Gratings* (Springer, Berlin, 1986), Chap. 2, p. 4.

²P. Andrew and W.L. Barnes, *Science* **306**, 1002 (2004).

³P. A. Hobson, J. A. E. Wasey, and W. L. Barnes, *IEEE J. Sel. Top. Quantum Electron.* **8**, 378 (2002).

⁴J. Vuckovic, M. Loncar, and A. Scherer, *IEEE J. Quantum Electron.* **36**, 1131 (2000).

⁵J. R. Lakowicz, *Anal. Biochem.* **324**, 153 (2004).

⁶P. N. Prasad, *Introduction to Biophotonics* (Wiley-Interscience, New York, 2003), Chap. 9, p. 311.

⁷B. Eegins, *Biosensors: An Introduction* (Wiley, New York/Teubner, Leipzig, 1996), Chap. 3, 31.

⁸E. F. Schubert, Y. H. Wang, A. Y. Cho, L. W. Tu, and G. J. Zidzik, *Appl. Phys. Lett.* **60**, 921 (1992).

⁹H. Benisty, H. De Neve, and C. Weisbuch, *IEEE J. Quantum Electron.* **34**, 1612 (1998).

¹⁰P. K. Tien, *Rev. Mod. Phys.* **49**, 361 (1977).

¹¹H. Hasegawa and H. L. Hartnagel, *J. Electrochem. Soc.* **123**, 713 (1976).

¹²R. J. Warmack and S. L. Humphrey, *Phys. Rev. B* **34**, 2246 (1986).

¹³J. L. Stanford, *J. Opt. Soc. Am.* **60**, 49 (1970).

¹⁴H. Raether, in *Surface Polaritons*, edited by V. M. Agranovich and D. L. Mills (North-Holland, Amsterdam, 1982), Chap. 9, p. 352.